ELSEVIER

Journal of Chromatography A, 952 (2002) 239–248

JOURNAL OF CHROMATOGRAPHY A

www.elsevier.com/locate/chroma

Kinetic study of the polymerization of α-amino acid *N*-carboxyanhydrides in aqueous solution using capillary electrophoresis

R. Plasson, J.Ph. Biron, H. Cottet*, A. Commeyras, J. Taillades

Laboratoire Organisation Moléculaire, Évolution et Matériaux Fluorés, UMR 5073, Université Montpellier II, CC17, Place E. Bataillon, 34095 Montpellier Cedex 5, France

Received 24 September 2001; received in revised form 27 December 2001; accepted 28 December 2001

Abstract

N-Carboxyanhydrides of amino acids (NCAs) are very reactive monomers able to polymerize into oligopeptides. They are assumed to be prebiotic precursors of the first polypeptides. Few reports have been published on the study of NCA polymerization in aqueous solution. In this work, a kinetic study focused on the hydrolysis of NCA and its coupling with amino acids and homopeptides (up to tripeptide) was carried out, taking L-valine derivatives as model compounds. For that purpose, capillary electrophoresis appeared to be an effective and reliable technique for the measurement of the kinetic constants. The electrophoretic separation conditions, the procedure for stopping NCA reactivity, as well as the conditions of reaction are discussed in detail. We report the variation of the kinetic constant of the coupling reaction of the NCA of valine with an oligovaline as a function of its degree of polymerization. Finally, a temperature study also allowed us to estimate the activation energies associated with the NCA of valine hydrolysis and its coupling reaction with valine.

Keywords: Kinetic studies; Activation energy; Amino acids; α-Amino acid *N*-carboxyanhydrides; Peptides; Valine

1. Introduction

For several decades, since Miller's experiment [1], prebiotic chemistry has evolved significantly. Many studies have reported clues of how the molecular components of living organisms may have been synthesized abiotically. Actually, most fundamental biomolecules (amino acids [2], purines [3], oses [4], etc.) can potentially be produced in the absence of life, either on Earth or in space.

However, life relies on huge molecular complexity. The problem comes down to understanding how the first polymers were synthesized from prebiotic monomeric subunits. More precisely, this work concentrates on amino acid self-polymerization, the key to understanding how the first oligopeptides could have been produced from a pool of monomeric subunits.

In previous work, it has been shown that α-amino acid *N*-carboxyanhydrides (NCAs) may have been

*Corresponding author. Tel.: +33-4-6714-3427; fax: +33-4-6763-1046.

E-mail address: hcottet@univ-montp2.fr (H. Cottet).

0021-9673/02/$ – see front matter
PII: S0021-9673(02)00018-3

good candidates as prebiotic monomeric subunits [5]. Indeed, they can be obtained under primitive conditions via amino acid carbamoylation and nitrosation [6]. They are very reactive amino acid derivatives, promptly hydrolyzing to give amino acids and polymerizing into oligopeptides as soon as they are placed in aqueous solution, particularly under prebiotic conditions (i.e. highly carbonated oceans [7]).

In order to understand the prebiotic chemistry of NCAs as a whole, a precise knowledge of the hydrolysis/polymerization process is necessary. However, very few kinetic studies of the aqueous polymerization of NCAs leading to the measurement of the kinetic constants have been reported [8,9]. Other works dealing with NCA polymerization in aqueous solution were focused on the characterization of the oligopeptides produced, either by using high-performance liquid chromatography [10], or liquid chromatography–mass spectrometry [11]. Furthermore, kinetic studies of NCA polymerization in aqueous or organic media were generally mostly focused on NCA consumption, monitored either by infrared detection [12], or by the resulting CO_2 production measured by manometric [8,9,13] or conductimetric [14] methods.

The purpose of this work was to examine all the kinetic aspects involved in the reactivity of NCA in buffered aqueous solution taking the NCA of L-valine as a model compound. Capillary electrophoresis (CE) appeared to be an appropriate separation technique for this purpose. Indeed, CE was the method of choice for the separation and quantification of the different species produced from the reaction of NCA in aqueous solution [15,16]: namely, amino acids and oligopeptides. The great potential of CE as a separation technique for the characterization of peptides has been extensively demonstrated, as illustrated by the numerous reviews on this subject [17–21]. CE separation and the electrophoretic behavior of homopolypeptides such as oligoalanines and oligoglycines have been studied in detail by Survay et al. [22,23]. In this work, the electrophoretic separation conditions were first studied for an optimal monitoring of NCA hydrolysis and polymerization. Furthermore, a kinetic study of the hydrolysis of the NCA of valine and its coupling with the first oligomers (valine, di- and trivaline) was carried out.

2. Theoretical

All the reactions studied follow the general scheme [24] described below:

$$Y \xrightarrow{k_h} X_1 \tag{1}$$

$$Y + X_i \xrightarrow{k_i} X_{i+1} \tag{2}$$

where k_h and k_i are the kinetic constants of each reaction step assuming that they are first-order reactions [8]. The first step (Eq. (1)) represents the hydrolysis of Y, the activated monomeric subunit, such as NCA. Y hydrolysis leads to X_1, the unactivated monomer, such as an amino acid. Other steps (Eq. (2)) represent the propagation of polymerization, namely the coupling between the Y activated monomer and X_i oligomer to form the X_{i+1} oligomer. i and $i+1$ ($i \geq 1$) are the degrees of polymerization (DPs) of the oligomers. The evolution of the concentrations of the different species present can be predicted by the following set of equations:

$$\dot{y} = -k_h y - \sum_{i \geq 1} k_i y x_i \tag{3a}$$

$$\dot{x_1} = k_h y - k_1 y x_1 \tag{3b}$$

$$\dot{x_i} = k_{i-1} y x_{i-1} - k_i y x_i \quad (i \geq 2) \tag{3c}$$

where y and x_i are, respectively, the concentrations of reactants Y and X_i. Usually, such equations cannot be solved easily nor exactly. Thus, approximations have to be made according to each initial experimental condition.

2.1. Hydrolysis of Y without any coupling

Initial experimental conditions are chosen so that all polymerization steps (i.e. Eq. (2)) are negligible in comparison with hydrolysis. This situation occurs for low concentrations of Y in the absence of X_i ($i \geq 1$). Eq. (3a) then reduces to:

$$\dot{y} = -k_h y \tag{4}$$

which leads to the following solution:

$$\frac{y}{y_0} = e^{-k_h t} \tag{5}$$

where y_0 is the initial concentration of the Y acti-

vated monomer. An estimation of the hydrolysis kinetic constant can be obtained by plotting the logarithm of the left-hand side of Eq. (5) as a function of time and by calculating the slope of the resulting straight line.

2.2. Hydrolysis of Y and coupling with X_n

Initial conditions are chosen such that all coupling steps are negligible except for the n^{th} one (i.e. Eq. (2) negligible for $i \neq n$). This amounts to adding to the reactor low concentrations of Y with an excess of X_n, which implies in terms of concentrations $x_n \gg y$. Thus, it can be considered that $x_n \simeq x_{n,0}$ (where $x_{n,0}$ is the initial concentration of X_n). Eq. (3a) then becomes:

$$\dot{y} = -(k_h + k_n x_{n,0})y \tag{6}$$

Mathematically, this latter equation is similar to Eq. (4), and the expression of y/y_0 will be comparable to Eq. (5), substituting k_h by $k_{app} = k_h + k_n x_{n,0}$:

$$\frac{y}{y_0} = e^{-(k_h + k_n x_{n,0})t} = e^{-k_{app}t} \tag{7}$$

The linearization of this equation yields an estimation of the apparent kinetic constant k_{app}. Furthermore, by measuring k_{app} for different $x_{n,0}$ concentrations, k_n can be derived from the slope of the line obtained by plotting k_{app} as a function of $x_{n,0}$. Inserting the value of y given by Eq. (7) into Eq. (3c) for $i = n + 1$ yields:

$$\dot{x}_{n+1} = k_n x_{n,0} y_0 \, e^{-k_{app}t} \tag{8}$$

Initially, $x_{n+1,0} = 0$ and the following expression can be derived from Eq. (8):

$$\frac{x_{n+1,\infty} - x_{n+1}}{x_{n+1,\infty}} = e^{-k_{app}t} \tag{9}$$

where $x_{n+1,\infty}$ is the asymptotic concentration of x_{n+1} for infinite time. Plotting the logarithm of the left-hand side of Eq. (9) versus t allows us to obtain another estimation of k_{app} from the measurement, on the graph, of the slope of the straight line. This latter estimation of k_{app} should be advantageously compared with the previous one obtained using Eq. (7), and, thus, should give some credence to our experimental method.

2.3. Influence of pH on k_i

The coupling reaction between X_i and Y is due to a nucleophilic attack on Y by the deprotonated form of the amine end group of X_i. Thus, k_i is a highly pH-dependent kinetic constant. The higher the pH value, the larger the kinetic constant k_i, due to the greater content of the X_i deprotonated form in the reaction medium. To go further in the modeling of the pH dependence of k_i, it is of interest to calculate $k_{i,corr}$, the intrinsic reaction constant relative to the active deprotonated form of X_i. $k_{i,corr}$ can be calculated by dividing k_i by the molar fraction of the active form present in the reaction medium:

$$k_{i,corr} = k_i \frac{x_i^a + x_i^b}{x_i^b} \tag{10}$$

where x_i^a and x_i^b are, respectively, the molar concentration of the acidic (i.e. protonated on its amine end group) and the basic form of X_i. Introducing the pK_a of the amine end group of X_i, Eq. (10) leads to:

$$k_{i,corr} = k_i(1 + 10^{pK_a - pH}) \tag{11}$$

From this latter equation and using the experimental determination of k_i at a given pH, an estimation of $k_{i,corr}$ can be made. Furthermore, knowing $k_{i,corr}$ and assuming that there is no catalytic buffer effect, the same equation can theoretically allow us to estimate the kinetic constant k_i whatever the pH value.

3. Experimental

3.1. CE instrumentation

Electrophoresis experiments were performed using an automated CE apparatus (Beckman P/ACE MDQ, Fullerton, CA, USA) with a positive polarity on the inlet side of the capillary. A fused-silica capillary—30 cm (20 cm to the detector)×50 μm I.D.—was initially conditioned with sodium hydroxide (0.1 *M* for 15 min under a pressure of 20 p.s.i.; 1 p.s.i. = 6894.76 Pa). Prior to analysis, the capillary was washed with 0.1 *M* phosphoric acid (20 p.s.i. for 2 min) and background electrolyte (20 p.s.i. for 3 min).

Furthermore, each four runs, the capillary was flushed with 0.1 *M* sodium hydroxide for 10 min under a pressure of 20 p.s.i. in order to remove adsorbed compounds. The capillary was thermostated at 25.0 °C. Samples were introduced hydrodynamically by the application of a positive pressure of 0.3 p.s.i. for 3 s (≈3.5 nl of sample injected, ≈1% of the capillary volume). Reaction products from NCA hydrolysis and polymerization were monitored spectrophotometrically at 214 nm. The experiments were carried out applying a constant voltage of 15 kV. The background electrolyte was 50 m*M* phosphoric acid containing 50 m*M* sodium chloride, and adjusted to pH 2.50 with pulverized pure NaOH.

3.2. Chemicals

The NCA of L-valine was synthesized by reaction of a gaseous NO/O_2 mixture with a suspension of carbamoylvaline in acetonitrile [6]. Carbamoylvaline was synthesized beforehand from the carbamoylation of valine with KNCO [25]. White pure crystals of NCA were obtained after recrystallization in ethyl acetate–hexane. The purity of the NCA was checked by nuclear magnetic resonance. Moreover, a fast atomic bombardment ionization mass spectrometry experiment was performed to check for the absence of residual ionic impurities such as NO_2^- or NO_3^-, which can potentially come from NCA synthesis. The NCA of valine could be kept under a nitrogen atmosphere at −16 °C for a few months without any observable degradation.

L-Valine (Val) was obtained from Acros (Geel, Belgium), di-L-valine (Val_2) and tri-L-valine (Val_3) from Bachem (Bubendorf, Switzerland), phenyltrimethylammonium chloride (PTMA) and *p*-methoxybenzylamine (MBzA) from Avocado (Heysham, UK), sodium dihydrogenphosphate (NaH_2PO_4) from Merck (Darmstadt, Germany) and phosphoric acid (H_3PO_4, 99.999% purity, 85%, w/w, in water) from Aldrich (Milwaukee, WI, USA). Purified water delivered by a Milli-Q system (Millipore, Molsheim, France) was used in all experiments except for organic synthesis, where deionized water was sufficient.

3.3. Monitoring method

The reaction medium was composed of 10 ml of a 0.1 *M* sodium dihydrogenphosphate solution containing 0 to 0.2 *M* valine or oligovaline and 20 m*M* PTMA (internal standard), adjusted to pH 6.00 with pulverized pure NaOH. The reaction cell was thermostated at an accurate temperature (±0.1 °C) in the 0–15 °C range. At time $t = 0$, 25–100 μl of a 50 g l^{-1} NCA solution in acetonitrile was quickly added to the thermostated reaction cell, rather than introducing pure NCA crystals. Indeed, slow NCA dissolution was observed when it was not dissolved beforehand in acetonitrile.

At various time intervals, from 30 s to 60 min depending on the reaction rate, 200 μl of the reaction cell were taken and mixed under stirring to 100 μl of

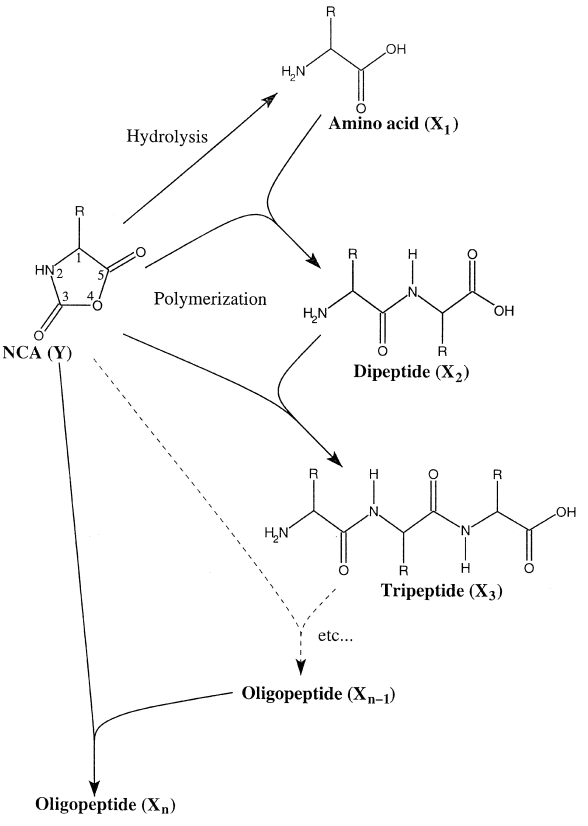

Fig. 1. Chemical structures of the compounds obtained by hydrolysis or polymerization of NCA.

0.2 *M* MBzA solution in water to stop the NCA reactivity. The samples were then analyzed by CE.

4. Results

As depicted in Fig. 1, NCA (*Y*) can either be hydrolyzed to an amino acid or be coupled with an X_{n-1} oligopeptide to form the X_n oligomer. This set of reactions is due to nucleophilic attack on C_5. It is worth noting that other reactions of NCAs, involving deprotonation of the nitrogen of the cycle, have been reported. As these latter reactions are mainly reported under basic and anhydrous conditions [26], they have been neglected here.

Because this work was limited to valine derivatives, the activated monomer *Y* (see Section 2) represents the NCA of valine ($R=CH(CH_3)_2$ in Fig. 1), while X_1 is valine and X_i is oligovaline ($DP=i$). All valine residues used in this study were L.

4.1. Optimization of the method for the monitoring of NCA hydrolysis and polymerization

4.1.1. Stopping NCA reactivity

To quantify the NCA contained in the thermostated reaction cell as a function of time, it was important to find a reactant able to stop the NCA reactivity. For that purpose, an excess of primary amine (*p*-methoxybenzylamine, MBzA) was added to the sample taken from the reaction cell (see Section 3.3). The reaction between the NCA of valine and the primary amine [27] is depicted in Fig. 2. This derivatization reaction of the NCA was also interesting in order to detect derivatized NCA by UV absorbance, thanks to the benzyl chromophore.

To check the quantitativity of the latter reaction, several volumes of 0.05 *M* MBzA solution in water were added to 100 μl of a 0.007 *M* solution of NCA. The time-corrected area corresponding to the derivatized NCA is plotted in Fig. 3 as a function of the number of equivalents of MBzA added to the sample. As seen from Fig. 3, the reaction was found to be quantitative above 10 equivalents of MBzA. In this work, for the monitoring of NCA reactivity, 100 μl of a 0.2 *M* MBzA solution (i.e. at least 15 equivalents of MBzA considering the highest initial NCA concentration) were added to stop the reaction occurring in the 200 μl sample taken from the reaction cell.

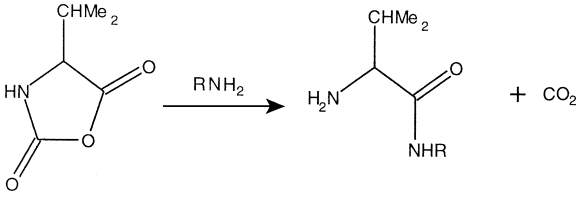

Fig. 2. Chemical reaction involved in the stopping of NCA reactivity ($R=MeO-Ph-CH_2-$).

4.1.2. CE method

CE conditions were optimized in order to separate and quantify all the compounds produced in the reaction cell. After the addition of MBzA to the sample taken from the reaction medium, the possible different molecules present were: NCA of valine derivatized by MBzA, MBzA in excess, oligovalines, valine, and, lastly, PTMA initially added to the reaction medium as an internal standard. PTMA was chosen because, as a quaternary ammonium, it has

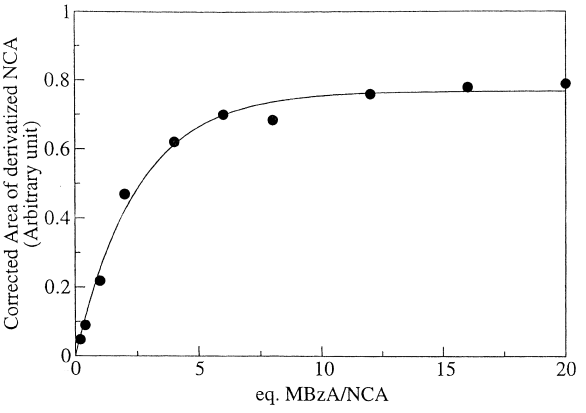

Fig. 3. Time-corrected areas of derivatized NCA as a function of the number of equivalents of MBzA added to the sample. Concentration of MBzA solution added to the NCA sample: 0.05 *M* in water. NCA concentration: 0.007 *M* in 0.1 *M* phosphate buffer, pH 6.0. Electrophoretic conditions, fused-silica capillary 30 cm (20 cm to the detector)×50 μm I.D.; electrolyte, 50 m*M* phosphoric acid buffer containing 50 m*M* sodium chloride, pH 2.50; applied voltage, +15 kV; current, 120 μA; hydrodynamic injection 0.3 p.s.i., 3 s (≈3.5 nl of sample injected, ≈1% of the capillary volume); UV detection at 214 nm; temperature, 25 °C.

no nucleophilic properties and cannot react with NCA. Furthermore, it is positively charged and has a good UV response due to the phenyl chromophore.

Optimal electrophoretic conditions were found to be 50 m*M* phosphate buffer, pH 2.5, containing 50 m*M* NaCl. Indeed, derivatized NCA, valine and oligovaline are positively charged at low pH. Oligopeptides bore an average positive charge of about 0.8–0.9 (see Table 1 for pK_a values), and were thus separated by their molecular masses—the larger the oligopeptide the slower its electrophoretic migration. Due to the lower acidic pK_a value, valine only had an average positive charge of 0.4, so that it has a slower electrophoretic migration in comparison with the first oligopeptides (DPs$\leq$5). The electrophoretic separation of all the species involved in this study, that is, in the order of increasing migration time: PTMA (internal standard), MBzA, NCA derivatized by MBzA, Val_2, Val_3, Val_4 and Val, is shown in Fig. 4.

Addition of NaCl to the electrolyte was found to avoid current instability and to limit the adsorption of amines onto the capillary silica wall. As the addition of salt induces an increase in the electrolyte conductivity, the applied voltage was reduced to 15 kV to avoid excessive heating of the capillary, or even current breakage.

Fig. 5 shows the evolution of the electropherograms obtained at different times for the coupling of NCA with valine. Experimentally, 0.0035 *M* NCA of valine was initially added in the reaction cell to a 0.1 *M* solution of valine in 100 m*M* phosphate buffer, pH 6.0. As expected, the area corresponding to the NCA (peak 3) decreases as it reacts with valine and also hydrolyzes, while peak 4, corresponding to divaline, increases in intensity. The fronting shape of valine (peak 5, Fig. 5) was likely due to adsorption on the capillary wall, since the peak shape was more symmetric for lower valine concentrations in the sample, as shown in Fig. 4.

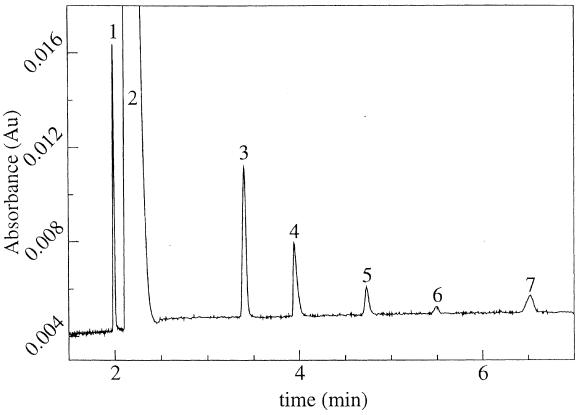

Fig. 4. Electrophoretic separation of the different species involved in this work. Experimental conditions: initial NCA concentration, 0.02 *M*; initial valine concentration, 0.1 *M*; 50 m*M* phosphate buffer, pH 6.0; temperature, 30 °C; reaction stopped by mixing 300 μl of 0.1 *M* MBzA with 100 μl of the reaction cell, at t = 3 min. Same electrophoretic conditions as in Fig. 3. Identification: 1, PTMA; 2, MBzA; 3, NCA derivatized by MBzA; 4, Val_2; 5, Val_3; 6, Val_4; 7, Val.

4.1.3. Calibration

Although measurements of the kinetic constants (k_h and k_i) did not require the calculation of absolute concentrations (see Section 2), the linearity of the calibration plot was verified with standard solutions. The calibration plots were linear using PTMA as an internal standard (10 m*M*) for standard solutions of valine (10 to 100 m*M*), derivatized NCA (1 to 10 m*M*) and divaline (0.3 to 2 m*M*) in the given concentration ranges. The corresponding correlation coefficients (R^2) calculated by least-squares regression were, respectively, 0.996, 0.998, and 0.999. The

Table 1
pK_a values of valine residues taken from the literature

	pK_a		Conditions	
	NH_3^+/NH_2	CO_2H/CO_2^-	Temp. (°C)	Ionic strength (m*M*)
Valine [28]	9.68	2.30	25	20–100
Val_2 [29]	7.97	3.39	25	100
Val in peptide[a] [30]	8.20	3.20	n.a.	n.a.

[a] Average value.

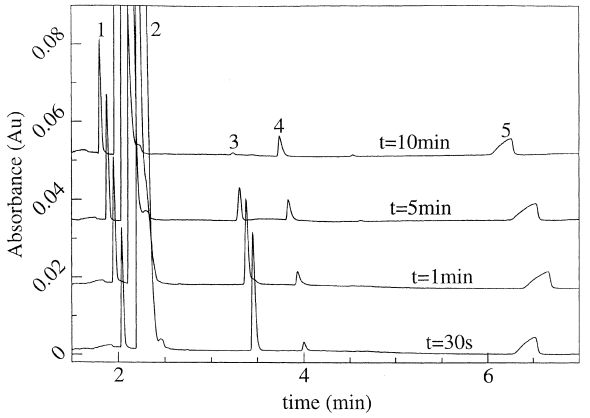

Fig. 5. Electropherograms obtained at different reaction times for the coupling of the NCA of valine with valine. Experimental conditions: initial NCA concentration, 0.0035 *M*; initial valine concentration, 0.1 *M*; 100 m*M* phosphate buffer, pH 6.0; temperature, 5 °C; reaction stopped by mixing 100 μl of 0.2 *M* MBzA with 200 μl of the reaction cell. Same electrophoretic conditions as in Fig. 3. Identification: 1, PTMA; 2, MBzA; 3, NCA derivatized by MBzA; 4, Val_2; 5, Val.

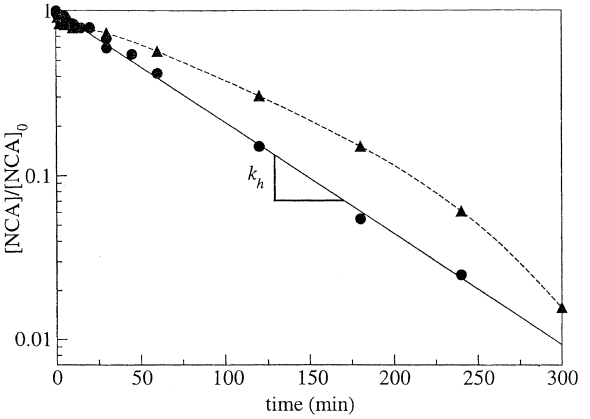

Fig. 6. Hydrolysis of the NCA of valine in aqueous solution with (●) and without (▲) phosphate buffer, pH 6. Experimental reaction conditions: 0.007 m*M* NCA of valine in pure water adjusted to pH 6 with HCl (▲) or in 100 m*M* phosphate buffer, pH 6 (β); temperature, 5 °C. Electrophoretic conditions: as in Fig. 3. For each experimental point, NCA contained in the sample was derivatized by an excess of MBzA (see text for details).

run-to-run precision ($n = 10$) of migration times and time-corrected area ratios relative to the internal standard (PTMA) was determined. Calculated values of the relative standard deviations (RSDs) are reported in Table 2. The RSD values for the migration times are good and those for time-corrected ratios are correct. On the whole, the best run-to-run precision was obtained for derivatized NCA.

4.1.4. Optimization of reaction conditions

In the case of NCA hydrolysis and according to Eq. (5), the plot of the logarithm of NCA concentration versus reaction time should yield a straight line of slope $-k_h$. As shown in Fig. 6, important deviations from linearity were obtained in non-buffered reaction medium containing only NCA of valine at $t = 0$. The deviations reported here were due to pH changes since the measured pH was not stable (±0.5 pH units) during NCA hydrolysis. Although the final pH was identical to the starting pH, pH changes occur during the reaction, due to the release of acidic and basic species, as already reported for the mechanism of NCA hydrolysis and polymerization [24]. In order to keep the pH and reaction rate stable, 100 m*M* phosphate buffer, pH 6.0, was added to the reaction medium. Under such conditions, no pH variations could be detected with a pH meter and the corresponding graph in Fig. 6 is linear ($R^2 = 0.997$). In all NCA hydrolysis or polymerization experiments of this work, the previously described buffer was used.

Table 2
Relative standard deviations of migration times and time-corrected area ratios (A/A_{ref}) relative to PTMA. Derivatized NCA concentration, 0.007 m*M*; valine concentration, 0.1 *M*; Val_2 concentration, 2 m*M*. Electrophoretic conditions as in Fig. 3

	Val_2	Val	Derivatized NCA-Val
RSD migration times (%)	0.4	3.4	1.0
RSD A/A_{ref} (%)	4.5	4.1	2.5

Further, to measure k_n, the kinetic constant associated with the coupling between the NCA of valine and Val_n, NCA had to be initially added at low concentration to a buffered solution containing an excess of Val_n.

4.2. Determination of k_h

To determine k_h, the first step in this kinetic study, conditions where no polymerization step occurs had to be found. Adding only NCA to the reaction medium consisting of phosphate buffer at pH 6 may

be insufficient to avoid the first coupling step, since amino acid produced by NCA hydrolysis may react with NCA to form divaline. To avoid the formation of divaline, low initial concentrations of NCA (i.e. ≤ 0.01 *M*) were used. In 0.1 *M* phosphate buffer at pH 6.0, no divaline formation was observed by CE as long as the temperature did not exceed 15 °C. Under such conditions, 99% of NCA was hydrolyzed typically in 5 h, which is sufficiently slow to allow the measurement of the evolution of the NCA concentration.

The evaluation of k_h was performed at 5 °C by plotting $\ln(y/y_0)$ as a function of time (Fig. 6) and by measuring the slope of the resulting line (see Eq. (5) in the Theoretical section). It was found that $k_h = 0.0264$ min^{-1}, with a least-squares correlation coefficient of $R^2 = 0.996$. Bartlett et al. [8] reported the following equation giving the hydrolysis kinetic constant for the NCA of glycine in acetate buffer, pH 4.76, at a constant 1 *M* ionic strength and at 0 °C:

$$k\,(\text{min}^{-1}) = 0.0168 + 0.0294[\text{AcO}^-] \quad (12)$$

where $[\text{AcO}^-]$ is the acetate molar concentration in *M*. As far as the kinetic constants are comparable, since the nature of the NCA, the ionic strength and the pH are different, the two values are of the same order.

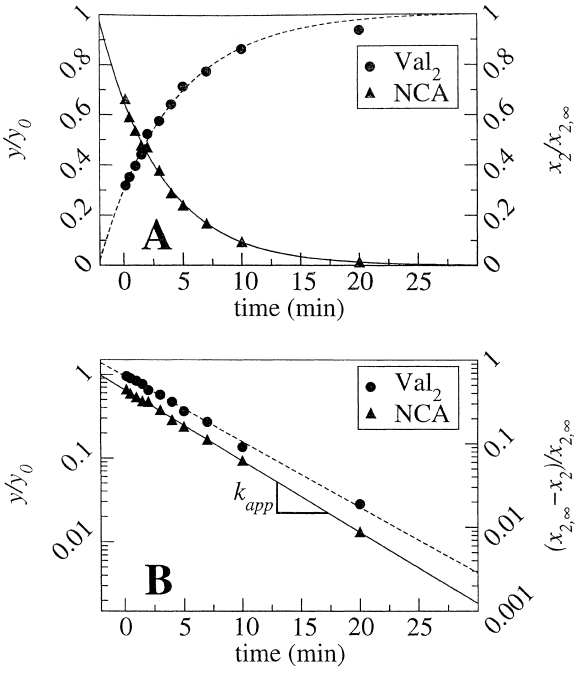

Fig. 7. Variation of y/y_0 (●) and $x_2/x_{2,\infty}$ (▲) on a linear scale (A) and y/y_0 (●) and $(x_{2,\infty} - x_2)/x_{2,\infty}$ (▲) on a logarithmic scale (B) during the reaction of the NCA of valine (*Y*) in the presence of valine (X_1). Experimental conditions: 0.2 *M* valine in 0.1 *M* phosphate buffer, pH 6.0; initial concentration of NCA of valine, 0.007 *M*; temperature, 5 °C. Electrophoretic conditions as in Fig. 3.

4.3. Determination of k_n

For the measurement of k_n, it was not possible to measure it directly since hydrolysis cannot be neglected whatever the chosen initial conditions. However, by mixing low NCA concentrations (i.e. ≤ 0.01 *M*) with an excess of X_n substrate (i.e. ≥ 7 equivalents of X_n relative to NCA), hydrolysis and NCA/X_n coupling were the only two reactions to take into account. Other coupling steps were assumed to be negligible since no X_i ($i \geq n+2$) oligomers were detectable by CE. Under these conditions, the ratios y/y_0 and $(x_{n+1,\infty} - x_{n+1})/x_{n+1,\infty}$ were expected to follow Eq. (7) and Eq. (9), respectively.

Fig. 7A shows the variation of the ratios y/y_0 and $x_{n+1}/x_{n+1,\infty}$ on a linear scale, and Fig. 7B gives the variation of the ratios y/y_0 and $(x_{n+1,\infty} - x_{n+1})/x_{n+1,\infty}$ on a logarithmic scale as a function of the reaction time in the case of NCA coupling with valine. At pH 6, 5 °C and in the presence of valine, 99% of the NCA of valine typically reacted in less than half an hour. As described in Section 2.2, the slopes obtained on the logarithmic scale give an estimation of the apparent kinetic constant $k_{\text{app}} = k_h + k_1 x_{1,0}$. Table 3 gathers all the obtained k_{app} values for different initial NCA concentrations. In accordance with theory, for a given initial valine concentration, k_{app} was found to be roughly independent of the initial NCA concentration. Further, by plotting k_{app} as a function of the initial valine concentration, a least-squares linear regression leads to $k_h = 0.0267$ min^{-1} and $k_1 = 0.988$ min^{-1} *M*$^{-1}$ ($R^2 = 0.996$). This latter k_h value is in good agreement with that previously obtained in Section 4.2, which gives additional credibility to the validity of the kinetic model.

The same procedure was used for the determi-

Table 3
Apparent kinetic constant k_{app} (min^{-1}) for different initial concentrations of the NCA of valine (y_0) and of oligovalines ($x_{i,0}$, $i \leq 3$). The least-squares correlation coefficients (R^2), each calculated on 12 experimental points, are given in parentheses. Reaction conditions: 0.1 *M* phosphate buffer, pH 6; temperature, 5 °C. Electrophoretic conditions as in Fig. 3

		y_0		
		0.00175 *M*	0.0035 *M*	0.007 *M*
$x_{1,0}$	0 *M*			0.0264 (0.996)
	0.05 *M*		0.0783 (0.997)	0.0795 (0.996)
	0.1 *M*		0.121 (0.998)	0.122 (0.999)
	0.15 *M*		0.179 (0.996)	0.172 (0.996)
	0.2 *M*	0.247 (0.998)	0.231 (0.999)	0.220 (0.995)
$x_{2,0}$	0.025 *M*	0.113 (0.996)		
	0.05 *M*		0.204 (0.991)	
$x_{3,0}$	0.02 *M*	0.108 (0.981)		
	0.05 *M*		0.220 (0.995)	

nation of k_2 and k_3. The corresponding k_{app} values with the calculated correlation coefficients are given in Table 3. The estimated values of k_n ($n \leq 3$) are derived from the linearization of k_{app} values and are listed in Table 4. It appears from these values that there is a great difference between k_1 and $k_{i\geq 2}$. This can be explained by the variations of the $pK_{a(NH_3^+/NH_2)}$ values with DP. Indeed, the $pK_{a(NH_3^+/NH_2)}$ value is lower for oligovaline than for valine (see Table 1). Thus, at pH 6, larger contents of the deprotonated form are present in the reaction medium in the case of oligovaline than for valine. As a consequence, the coupling with the NCA occurs more quickly in the case of oligovaline. The values of k_2 and k_3 are of the same order since the corresponding pK_a values are similar.

In order to take into account the influence of the difference in the pK_a values on the reactivity, k_i values were corrected according to Eq. (11). The corresponding $k_{i,corr}$ intrinsic kinetic constants are reported in Table 4. It should be noted that these values are only rough estimations, since pK_a values are given at 25 °C and 100 m*M* ionic strength while the reaction was performed at 5 °C and 115 m*M* ionic strength. In addition, the exact pK_a value in the case of trivaline was not available. Nevertheless, it was found that oligovaline is, intrinsically (8 to 15 times), less reactive than valine. Similar ratios for the intrinsic kinetic constants, ranging between 8 and 12, were previously reported for oligoglycine (DP≤3) [3].

Table 4
Kinetic constants k_i and intrinsic kinetic constant $k_{i,corr}$ for the coupling of the NCA of valine with Val_i ($i \leq 3$) at pH 6 and 5 °C. k_i values were calculated by linearization of the data given in Table 3 (see text and Section 2 for more details). $k_{i,corr}$ values were calculated using Eq. (10)

i	k_i ($min^{-1}\ M^{-1}$)	R^2	$k_{i,corr}$ ($min^{-1}\ M^{-1}$)
1	0.988	0.996	4730
2	3.55	0.999	335
3	3.86	0.999	364[a]
			615[b]

[a] Evaluated value taking $pK_a = pK_{a(Val_2)}$ in Table 1.
[b] Evaluated value taking $pK_a = pK_{a(Val\ in\ peptide)}$ in Table 1.

4.4. Determination of activation energies (E_a)

In order to be able to evaluate the kinetic constants at any temperature, an estimation of the activation energies was performed in the case of the NCA of valine hydrolysis and its coupling with valine. Table 5 displays the calculated kinetic constants at different temperatures, measured in 0.1 *M* phosphate buffer, pH 6. These values were found to follow the Arrhenius law, and the relative activation energies were calculated by plotting the logarithm of the kinetic constant versus T^{-1} (graph not shown). $E_a(k_h) = 61$ kJ mol^{-1} ($R^2 = 0.999$) and $E_a(k_1) = 55$ kJ mol^{-1} ($R^2 = 0.999$), respectively, were calculated

Table 5
Kinetic constants for the NCA of valine hydrolysis and its coupling with valine at different reaction temperatures

Temp. (°C)	k_h (R^2)[a] (min^{-1})	k_1 (R^2)[b] ($min^{-1}\ M^{-1}$)
0	0.0178(0.998)	0.644(0.998)
5	0.0264(0.996)	0.988(0.996)
10	0.0467(0.997)	1.513(0.998)
15	0.0720(0.999)	

[a] NCA of valine concentration, 0.0035 *M*.
[b] NCA of valine concentration, 0.0035 *M*; valine concentration, 0.1 *M*. k_1 was determined using the equation $k_{app} = k_h + k_1 x_{1,0}$ and after the experimental determination of k_h under the same conditions. Other experimental conditions were the same as in Table 3.

by least-squares regressions for the hydrolysis of NCA and its first step coupling with valine.

5. Conclusion

In this work, capillary electrophoresis was found to be a useful and reliable separation technique for studying the kinetic aspects of NCA hydrolysis and polymerization in aqueous solution. Indeed, after determination of the NCA hydrolysis kinetic constant, it was possible to estimate the kinetic constants k_i of the coupling of NCA with the first oligopeptides (up to tripeptide) in the case of L-valine derivatives. Activation energies corresponding to k_h and k_1 were also evaluated successfully. It was demonstrated that k_i increases by a factor of 3 to 4 from k_1 to k_i ($i \geq 2$). This increase in reactivity of the NCA with the amino acid, on the one hand, and with the first oligopeptides, on the other, was explained qualitatively by the differences in the $pK_{a(NH_3^+/NH_2)}$ values. However, to gain a better insight into the dependence of k_i ($i \geq 1$) on pH, it would be very interesting to measure the exact pK_a values of the valine derivatives under the same conditions as the reaction. In this way, it should be possible to anticipate the k_i values whatever the pH and to compare these values with the experimental values in order to assess the kinetic model. Another important perspective in prebiotic chemistry would be to study, using this approach, the stereoselectivity in NCA reactivity, as it may explain the emergence of the homochirality of proteins [11,31]. Future work will be performed in these directions.

References

[1] S.L. Miller, Science 117 (1953) 528.
[2] J. Taillades, I. Beuzelin, L. Garrel, V. Tabacik, C. Bied, A. Commeyras, Orig. Life Evol. Biosph. 28 (1998) 61.
[3] J. Oró, A.P. Kimball, Arch. Biochem. Biophys. 94 (1961) 217.
[4] D. Müller, S. Pitsh, A. Kittaka, E. Wagner, C.E. Wintner, A. Eschenmoser, Helv. Chim. Acta 73 (1990) 1410.
[5] J. Taillades, H. Collet, L. Garrel, I. Beuzelin, L. Boiteau, H. Choukroun, A. Commeyras, J. Mol. Evol. 48 (1999) 638.
[6] H. Collet, C. Bied, L. Mion, J. Taillades, A. Commeyras, Tetrahedron Lett. 37 (1996) 9043.
[7] Kasting, Orig. Life Evol. Biosph. 27 (1993) 291.
[8] P.D. Bartlett, D.C. Dittmer, J. Am. Chem. Soc. 79 (1957) 159.
[9] P.D. Bartlett, R.H. Jones, J. Am. Chem. Soc. 79 (1957) 2153.
[10] A.R. Hill, L.E. Orgel, Orig. Life Evol. Biosph. 26 (1996) 539.
[11] T. Hitz, M. Blocher, P. Walde, P.L. Luisi, Macromolecules 34 (2001) 2443.
[12] M. Idelson, E.R. Blout, J. Am. Chem. Soc. 79 (1957) 3948.
[13] S.G. Waley, J. Watson, Proc. R. Soc. London A 199 (1949) 499.
[14] R.D. Lundberg, P. Doty, J. Am. Chem. Soc. 79 (1957) 3961.
[15] P.G. Righetti, Capillary Electrophoresis in Analytical Biotechnology, CRC Press, Boca Raton, FL, 1996.
[16] P.D. Grossman, J.C. Colburn, Capillary Electrophoresis: Theory and Practice, Academic Press, San Diego, CA, 1992.
[17] N.J. Adamson, E.C. Reynolds, J. Chromatogr. A 699 (1997) 133.
[18] A. Cifuentes, H. Poppe, Electrophoresis 18 (1997) 2362.
[19] H.J. Issaq, Electrophoresis 21 (2000) 1921.
[20] V. Kasicka, Electrophoresis 20 (1999) 3084.
[21] C.K. Larive, S.M. Lunte, M. Zhong, M.D. Perkins, G.S. Wilson, G. Gokulrangan, T. Williams, F. Afroz, C. Schöneich, T.S. Derrick, C.R. Middaugh, S. Bogdanowich-Knipp, Anal. Chem. 71 (1999) 389R.
[22] M.A. Survay, D.M. Goodall, S.A.C. Wren, R.C. Rowe, J. Chromatogr. 636 (1993) 81.
[23] M.A. Survay, D.M. Goodall, S.A.C. Wren, R.C. Rowe, J. Chromatogr. A 741 (1996) 99.
[24] M. Dvořák, F. Rypáček, Chem. Listy 89 (1995) 423.
[25] J. Taillades, L. Boiteau, I. Beuzelin, O. Lagrille, J.-P. Biron, W. Vayaboury, O. Vandenabeele-Trambouze, O. Giani, A. Commeyras, J. Chem. Soc., Perkin Trans. 2 7 (2001) 1247.
[26] H.R. Kricheldorf (Ed.), α-Amino Acids–*N*-Carboxyanhydrides and Related Heterocycles, Springer, Berlin, 1987, p. 67.
[27] M. Frankel, E. Katchalski, J. Am. Chem. Soc. 65 (1943) 1670.
[28] D.D. Perrin (Ed.), Dissociation Constants of Organic Bases in Aqueous Solution, Butterworths, London, 1965, p. 404.
[29] A.Q. Lyons, L.D. Pettit, J. Chem. Soc., Dalton Trans. (1984) 2305.
[30] E.C. Rickard, M.M. Strohl, R.G. Nielsen, Anal. Biochem. 197 (1991) 197.
[31] Cs. Fajszi, J. Czégé, J. Theor. Biol. 88 (1981) 523.